THE UNSTEADY LIQUID FILM FLOW OF THE CARBON NANOTUBES ENGINE OIL NANOFLUID OVER A NON-LINEAR RADIALLY EXTENDING SURFACE

by

Abdullah K. ALZAHRANI[a], Malik Z. ULLAH[a], Taza GUL[b], and Dumitru BALEANU[c,d*]

[a] Department of Mathematics, King Abdul Aziz University, Jeddah, Saudi Arabia
[b] Department of Mathematics, City University of Science and Information Technology, Peshawar, Pakistan
[c] Department of Mathematics, Faculty of Arts and Sciences, Cankaya University, Ankara, Turkey
[d] Institute of Space Sciences, Magurele-Bucharest, Romania

Original scientific paper
https://doi.org/10.2298/TSCI190404275A

The enhancement of heat transfer through carbon material is the objective of this study. The renowned class of carbon identified as single walled carbon nanotubes and multi walled carbon nanotubes, nanofluid-flow over a non-linear and unstable surface has been explored. The thermophysical properties of the two sorts of carbon nanotube have been implemented from the experimental outputs in the existent literature using engine oil as a base fluid. The viscous dissipation term has also been included in the energy equation improve the heat transfer rate. The thickness of the nanofluid thin layer is kept variable under the influence of the unstable and non-linear stretching of the disk. The elementary governing equations have been transformed into coupled non-linear differential equations. The problem solution is achieved through BVP 2.0 package of the optimal homotopy analysis method. The square residual error for the momentum and thermal boundary-layers up to the 20th order approximations have been obtained. The numerical ND-solve method has been used to validate the he optimal homotopy analysis method results. The impact of the model parameters vs. velocity field and temperature distribution have been shown through graphs and tables. The impact of the physical parameters on the temperature profile and velocity, pitch for both multi wall carbon nanotubes and single walled carbon nanotubes is gained in the range of $0 \leq \phi \leq 4\%$. From the obtained results it is observed that the single walled carbon nanotubes nanofluids are more efficient to improve the heat transfer phenomena as compared to the multi wall carbon nanotubes.

Key words: *carbon nanotubes engine oil based nanofluid, magnetic field, non-linear flexible and unstable disc, viscouse dissipation, transfer rate, drag force and heat, optimal homotopy analysis method BVPh 2.0.*

Introduction

The carbon nanotube (CNT) is the most important class of carbon family, which have exceptional thermal, chemical, mechanical, electronic and optical properties. The astonishing properties of the CNT have positioned them quite important for the mechanical engineering and materials sciences. Oberlin *et al.* [1] were the pioneers to describe the TEM images of the

* Corresponding author, e-mail: dumitru@cankaya.edu.tr

CNT. Iijima [2] have investigated the tube-like nanosized CNT in diameter range 4-30 nm. The idea of single wall carbon nanotubes (SWCNT) was established by two research groups [3, 4].

Later on, this idea was more explained by To [5] to specify that the bending of graphene sheet in small nanosized known as CNT. This study also categorized CNT in its two core classes named SWCNT and multi wall carbon nanotubes (MWCNT). The size of the SWCNT is 1 nm while MWCNT is in the form of a cluster containing 2-50 concentric tubes with 0.34 nm spacing.

The imperative applications of CNT are mostly related to energy alteration, electronics and automotive. The CNT are in the metal shape and can improve electricity and heat transfer rate [6, 7]. The use of the CNT in the field of mechanical engineering EOR for the oil recovery was utilized by Negin *et al.* [8]. Nieto de Castro and Murshed [9] have studied the thermal properties of a special type of nanofluids called ionofluids. Inon-ofluids contain some exceptional property and due to this property concentration and temperature CNT increased. Zaidi *et al.* [10] Inspected nanofluid of CNT flow of wall jet streaming by means of the convective physical state using a numerical method.

The stable dispersion of CNT in various liquids accomplishes the CNT nanofluids. The useful base liquids which are suitable for the synthesis of CNT are water, ethylene glycol and engine oils. Various of the researchers [11-19] have utilized the aforementioned base fluids for the stable dispersion of CNT.

The diversities of models exhibit in the literature to describe the thermal conductivities of CNT in the varieties of structures. The efforts done by the researchers to define a comparative model for the improvement of the thermal conductivities of CNT are Maxwell [20], Jeffery [21], Davis model [22], Lu and Lin [23], and Hamilton and Crosser [24]. All the researchers have done the significant work for the enhancement of heat exchange by introducing the thermal conductivity models and these models are used for the various nanomaterials.

Xue [25] suggested a model of the for the suitable dispersion of CNT depending on the shape and properties of CNT.

In the past much attention has been paid to the steady flows over the linearly stretchable surfaces. Still a lot of work is required to be reported for the fluid-flow over an unsteady and non-linear stretched surfaces [26-29].

The liquid film diffusion has substantial applications in the arena of science and manufacturing. The uses of coating in different industries like fiber coating used for telecommunication purposes, coating of the sheets cylinder disc [30], *etc.* Recently, Gul [31] have examined the liquid film sprinkling over a non-linear enlarging surface. Ghanj [32], have studied the liquid film flow of non-Newtonian fluids using the oscillatry geometry. Gohar *et al.* [33] have reflected the steady flow of the CNT over a non-linear enlarging disc. They studied the SWCNT and MWCNT considering the steady flow of the water based nanofluid. Qasim *et al.* [34] conferred the unsteady flow of the thin nanoliquid layer using Buongiorno's model. The thin film spray of the nanofluid over an extending tube for the thermal and cooling applications has been studied by Wang [35] and Khan *et al.* [36]. Alshomrani and Gul [37] have extended the spray of a nanoliquid film over the slippery surface of an extending cylinder.

Keeping in mind the aforementioned meaningful work the purpose of the recent work to analyze the liquid film flow of a SWCNT/MWCNT engine oil based nanofluid-flow over an unstable and non-linearly extending surface. The solution of the transformed non-linear equations is achieved by a well-known analytical technique optimal homotopy analysis method (OHAM) [38, 39]. Advance version of this technique (BVP-2) has been used for the error analysis which authenticates the convergence of the obtained results. The MATHEMATICA Pack-

age BVPh 2.0 for non-linear boundary value problems has been adopted by Zhao *et al.* [40], and this package is frequently used for the high non-linear problems [41-43] in various engineering problems. Furthermore, the validation of this method has been checked by the researchers [44, 45] with the existing literature. The influence of the modeled different parameters under the influence of SWCNT/ MWCNT is calculated successfully.

Problem formulation

A thin film of SWCNT/MWCNT engine oil based nanofluids is considered over an unsteady and non-linearly extending disc. Initially the disc is positioned at $z = 0$ and $z = h$ is limited thickness of thin film nanofluid. The non-linear velocity $U_w = ar^h/(1 - bt)$ is used for the stretching of the disc. Where $n = 1$ represent the linear stretching and $n = 2, 3, 4...$, represent the extending non-linear disc. The radius of the disc is presented by r and t is the time. The magnetic field acts perpendicularly to the fluid-flow direction. Let us suppose that the pressure is atmospheric, on behalf of this pressure term is vanished. The continuity, momentum and energy equations for the unsteady nanofluid-flow are identified as:

$$\frac{\partial u}{\partial r}+\frac{u}{r}+\frac{\partial w}{\partial z}=0 \tag{1}$$

$$\rho_{\mathrm{nf}}\left(\frac{\partial u}{\partial t}+u\frac{\partial u}{\partial r}+w\frac{\partial u}{\partial z}\right)=\left(\mu_{\mathrm{nf}}\frac{\partial^2 u}{\partial z^2}-\sigma_{\mathrm{nf}}B_0^2 u\right) \tag{2}$$

$$(\rho Cp)_{\mathrm{nf}}\left(\frac{\partial T}{\partial t}+u\frac{\partial T}{\partial r}+w\frac{\partial T}{\partial z}\right)=\left[k_{\mathrm{nf}}\frac{\partial^2 T}{\partial z^2}+\mu_{\mathrm{nf}}\left(\frac{\partial u}{\partial z}\right)^2\right] \tag{3}$$

The initial and boundary conditions prepared for our model is given below:

$$u=U_w,\quad w=0,\quad \Theta=\Theta_w,\quad \text{at } z=0,\quad \mu\frac{\partial u}{\partial z}=\frac{\partial \Theta}{\partial z}=0,\quad w=\frac{\mathrm{d}h}{\mathrm{d}t},\quad \text{at } z=h \tag{4}$$

The stream function:

$$\psi(r,z)=-r^2U_w\,\mathrm{Re}^{-1/2}\,f(\eta)\quad\text{and}\quad \eta=\frac{z}{r}\mathrm{Re}^{1/2}$$

was used for the similarity transformation of the prevailing equations. The components of velocity are transformed as:

$$u=-\frac{1}{r}\frac{\partial\psi(r,z)}{\partial z}=U_w f'\ \text{ and }\ w=\frac{1}{r}\frac{\partial\psi(r,z)}{\partial r}=-U_w\,\mathrm{Re}^{-1/2}\left[\left(\frac{3+n}{2}\right)f+\left(\frac{n-1}{2}\right)\eta\frac{\mathrm{d}f}{\mathrm{d}\eta}\right]$$

along the radial and axial direction, respectively. Mathematically Reynold number in our model $\mathrm{Re} = rU_w/\nu_f$. The $T = T_0 - T_{\mathrm{ref}}(U_w^2/2a\,\nu_f)\Theta(\eta)$ is used for the transformation of the energy equation in which T_{ref}, signifies reference temperature. After applying the transformation temperature and velocity components in the eqs. (1)-(4) which satisfy the continuity equation and the rest of the equations have been attained:

$$f'''+(1-\phi)^{2.5}\left[(1-\phi)+\phi\frac{\rho_{\mathrm{CNT}}}{\rho_f}\right]\left[\left(\frac{3+n}{2}\right)ff''-n(f')^2-S\left(f'+\frac{\eta}{2}f''\right)\right]-(1-\phi)^{2.5}Mf'=0 \tag{5}$$

$$\frac{k_{\mathrm{nf}}}{k_f}\Theta+\mathrm{Pr}(1-\phi)^{2.5}\left[(1-\phi)+\phi\frac{(\rho C_p)_{\mathrm{CNT}}}{(\rho C_p)_f}\right]\left[\left(\frac{3+n}{2}\right)f\Theta-2n(\Theta f')\right]+(1-\phi)^{-2.5}\,\mathrm{Ec}\,\mathrm{Pr}(f')^2=0 \tag{6}$$

$$f(0)=0,\ f'(0)=1,\quad \Theta(0)=1,\quad f''(\beta)=0$$
$$\left(\frac{n+3}{2}\right)f(\beta)+\left(\frac{n-1}{2}\right)\beta f'(\beta)=\frac{S\beta}{2},\quad \Theta'(\beta)=0 \tag{7}$$

The model suggested by Xue [25] has been used due to great axial ratio and repaying the CNT space dispersal. The thermal conductivity of the CNT nanofluids has been calculated using this model as: in eq. (7) for linear stretching, $n = 1$, the conditions match to the published work [31].

The mathematical representation of the density of nanofluid is $\rho_{nf} = (1-\phi)\rho_f + \phi\rho_{CNT}$, where ρ_{CNT} indicates CNT density and ϕ show nanoparticle volume fraction. Dynamic viscosity of nanofluid is in the form of $\mu_{nf} = (1-\phi)^{10/25}$. Formula of kinematic viscosity used in our model can be written as $\nu_{nf} = \mu_{nf}(\rho_{nf})^{-1}$. The term $(\rho C_p)_{nf} = (1-\phi)(\rho C_p)_f + \phi(\rho C_p)_{CNT}$, denote the nanofluid capacity of specific heat specific heat. The $\beta = r^{-1}h\mathrm{Re}^{1/2}$, is the thin film thickness of the nanofluid.

The

$$M=\frac{r\sigma_{nf}B_0^2}{\rho_f U_w}=\frac{\sigma_f B_0^2(\rho_f a)}{r^{(n-1)}}$$

is the dimensionless magnetic field. The Prandtl number is represented by $\mathrm{Pr} = \mu_f C_p/k_f$ and $\mathrm{Ec} = U_w^2/(C_p)_f\Delta T$ is the Eckert number. The parameters used for engineering purposes are Nusselt number and skin fraction which can represent as $C_f = 2\tau_w/\rho_{nf}U_w^2$ and $\mathrm{Nu} = r^n q_w/k_{nf}\Delta T$, respectively.

The wall stress $\tau_\omega = \mu_f(\partial u/\partial z)_{z=0}$ and heat flux $q_w = k_{nf}(\partial T/\partial z)_{z=0}$ have been inserted to the discussed parameters as:

$$\frac{1}{2}\mathrm{Re}^{1/2}(1-\varphi)^{25/10}\sqrt{\left((1-\phi)+\phi\frac{\rho_{CNT}}{\rho_f}\right)}C_f=-f''(0),\quad \frac{\mathrm{Re}^{(-1)/2}(1-\varphi)^{20/25}}{\sqrt{\left[(1-\phi)+\phi\frac{\rho_{CNT}}{\rho_f}\right]}}\mathrm{Nu}=-\Theta'(0) \tag{8}$$

The OHAM-BVPh 2.0 package

The BVPh-2.0 package of OHAM [38-40] has been applied for the solution of the modeled eqs. (5) and (6) with the physical conditions in eq. (7).

The 20th order approximation has been obtained and the residual error has been minimized for the stable convergence of the obtained results. The resulting linear operators and initial trials which have an important role in the OHAM solution are selected as:

$$f_0(\eta)=\frac{1}{(3+5n)}\left[(3+5n)\eta-(2+2n-5)\right]\left(\frac{3}{\beta}\eta^2-\frac{1}{\beta^2}\eta^3\right),\quad \Theta_0(\eta)=1 \tag{9}$$

Suppose the linear operators λ_f and λ_Θ are defined as:

$$\lambda_f=\frac{\partial^4}{\partial\eta^4}\quad\text{and}\quad \lambda_\Theta=\frac{\partial^2}{\partial\eta^2} \tag{10}$$

Thus the common result of λ_f and λ_Θ is:

$$\lambda_f\left[\lambda_1+\lambda_2\eta+\lambda_3\eta^2+\lambda_4\eta^3\right]=0\quad\text{and}\quad \lambda_\Theta\left[\lambda_5+\lambda_6\eta+\lambda_7\eta^2\right]=0 \tag{11}$$

According to the essential information of OHAM clarified in [38, 40], eqs. (5) and (6) are validated as:

$$\varepsilon_m^f = \frac{1}{\lambda+1}\sum_{j=1}^{\lambda}\left\{\aleph_f\left[\sum_{i=1}^{m} f(\eta)\right]_{\xi=j\delta\xi}\right\}^2 \tag{12}$$

$$\varepsilon_m^\Theta = \frac{1}{\lambda+1}\sum_{j=1}^{\lambda}\left\{\aleph_\Theta\left[\sum_{i=1}^{m} f(\eta), \sum_{i=1}^{m}\Theta(\eta)\right]_{\xi=j\delta\xi}\right\}^2 \tag{13}$$

Liao [39, 40] was the first that defined total squared residual error using OHAM:

$$\varepsilon_m^t = \varepsilon_m^f + \varepsilon_m^\Theta \tag{14}$$

The auxiliary parameters have been used and the total residual error ε_m^t has been obtained from the velocity field and temperature distribution, respectively. The numerical values of the optimal convergence control parameters $h_f = -0.62701235$, $h_\Theta = -1.234102321$ have been archived in case of the SWCNT while has been obtained in the case of MWCNT. This method has the tendency to obtain the solution of the non-linear differential equation without discretization in short time with residual error. Due to this fact, this method is frequently used in the recent research [38-45]. Furthermore, the increasing order of approximation reduces the square residual error which leads to the close convergence of the problem.

The appropriate range of the physical parameters has also been calculated through OHAM and displayed. The obtained range of parameters for the proposed problem authenticates the convergence of the obtained results.

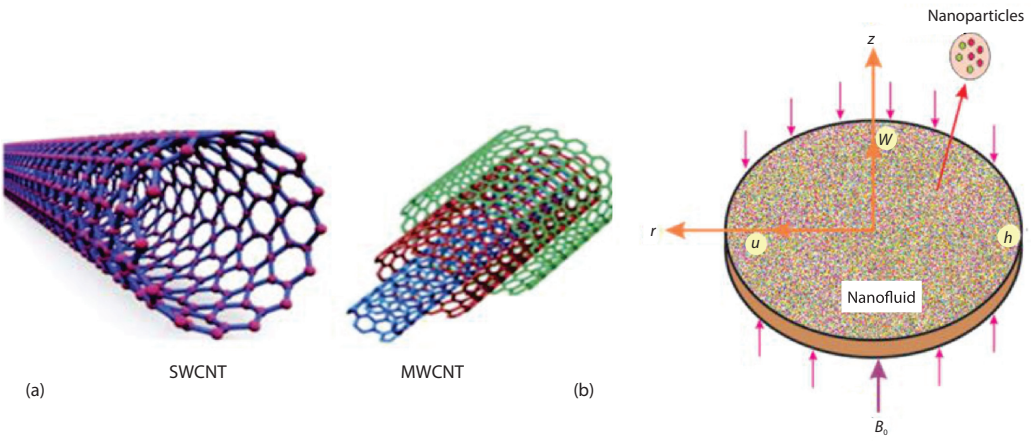

Figure 1. (a) The SWCNT and MWCNT, (b) physical interpretation of the problem

Results and discussion

The thin film flow of CNT nanofluid over an unstable and non-linear radially stretching disc have been concentrated in this research. The SWCNT/MWCNT engine oil based nanofluid has been utilized within the range $0 \le \phi \le 10\%$. The OHAM-BVPh-2.0 package has been used for the solution of the problem. Figure 1(a) display the shapes of SWCNT and MWCNT while fig. 1(b) shows the geometry of the problem. In fig. 2(a) the square residual error for the momentum and thermal equations are reflected using the BVPh-2.0 package. The convergence for the 30th order of the OHAM method have been calculated and from the residual error, it is

observed that the strong convergence has been started from the 20th iteration using the SWCNT. The 30th order convergence using the MWCNT has been obtained through the OHAM method and displayed in fig. 2(b). It is observed that the residual error analysis authenticates the strong convergence of the OHAM method at the 10th iteration.

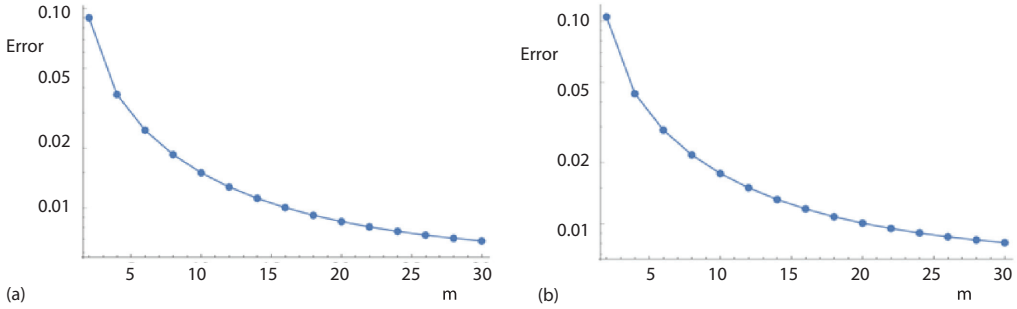

Figure 2. Total Residual error OHAM up to 30th order approximation of (a) the SWCNT, (b) the MWCNT

The suitable range of the physical parameters and their impact on the fluid motion have been illustrated in figs. 3-15.

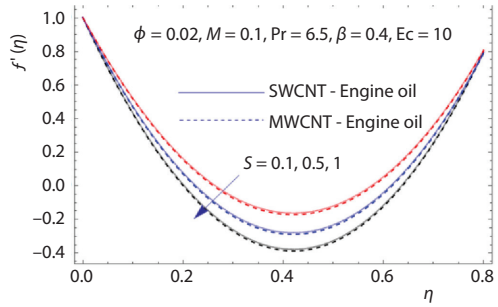

Figure 3. The impact of the unsteady parameter S on the velocity field $f'(\eta)$

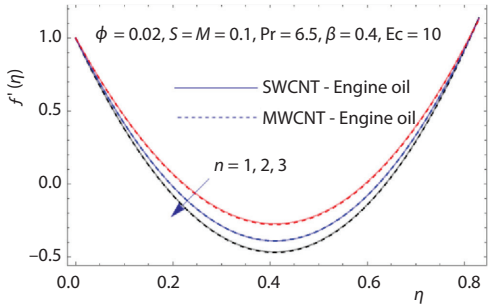

Figure 4. The impact of the non-linear stretching parameter n on the velocity field $f'(\eta)$

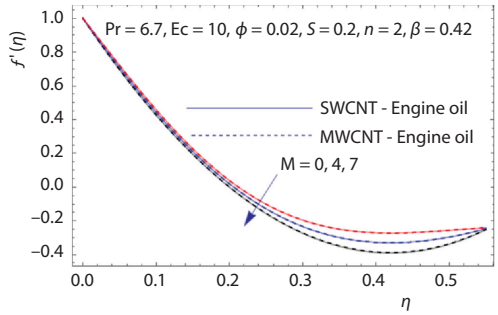

Figure 5. The impact of the magnetic parameter M on the velocity field $f'(\eta)$

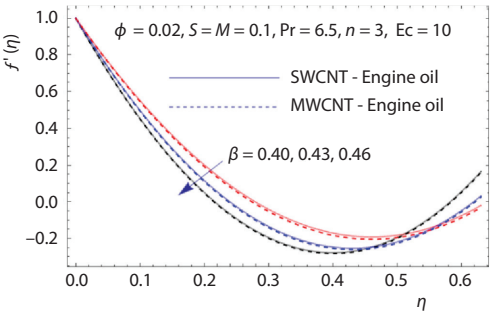

Figure 6. Thickness parameter β *vs.* $f'(\eta)$

The larger amount of the unsteady parameter, S, declines the velocity profile and this effect is shown in fig. 3. Since the higher values of S enhancing the resistive force cause drop the radial velocity. The stretching fact is occurring by accelerating the value of non-linearity,

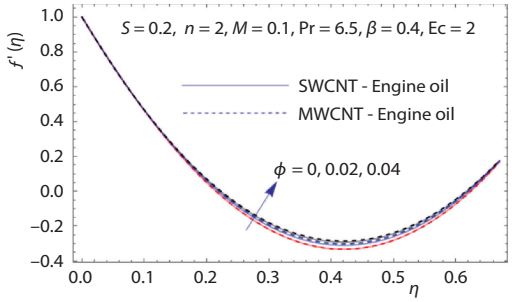

Figure 7. The ϕ *vs.* velocity field $f'(\eta)$

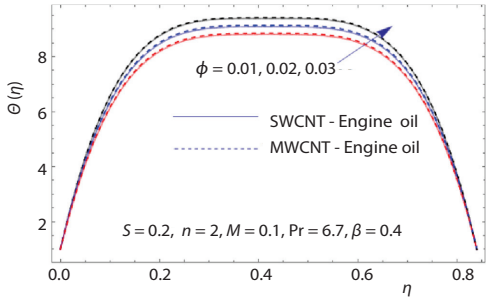

Figure 8. Nanoparticle volume fraction ϕ *vs.* $\Theta(\eta)$

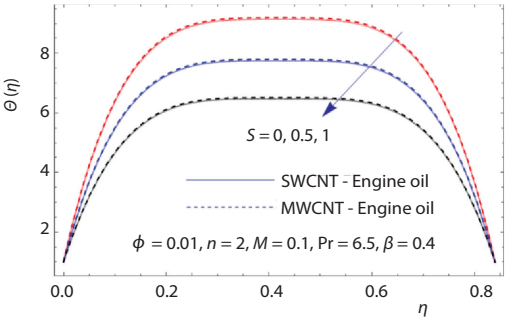

Figure 9. The impact of the unsteadiness parameter S on the temperature field $\Theta(\eta)$

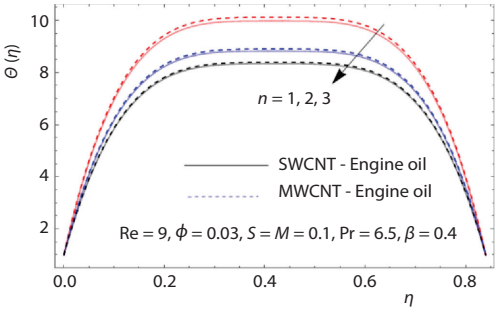

Figure 10. The impact of the non-linear stretching parameter n on the temperature field $\Theta(\eta)$

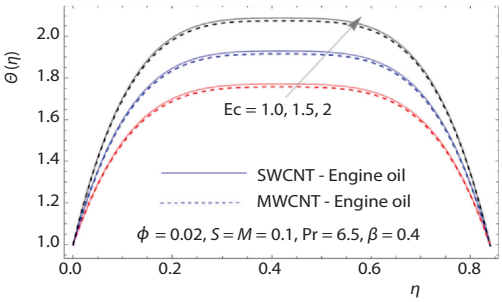

Figure 11. The impact of the Eckert number on the temperature field $\Theta(\eta)$

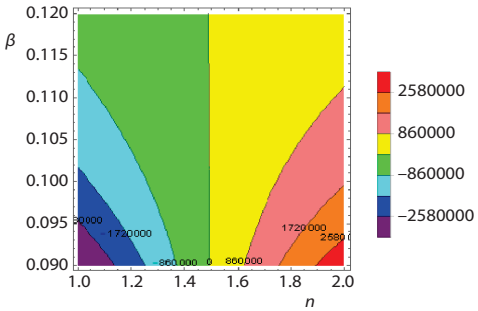

Figure 12. The β *vs.* n in the SWCNT, when $x = 3$, Pr = 10.7, $S = 0.3$, $M = 0.3$, and $\phi = 0.01$

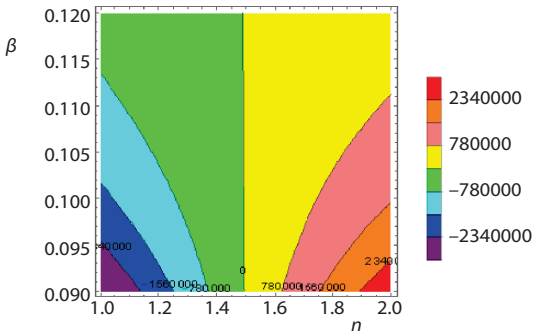

Figure 13. The β *vs.* n in MWCNT, when $x = 3$, Pr = 10.7, $S = 0.3$, $M = 0.3$, and $\phi = 0.01$

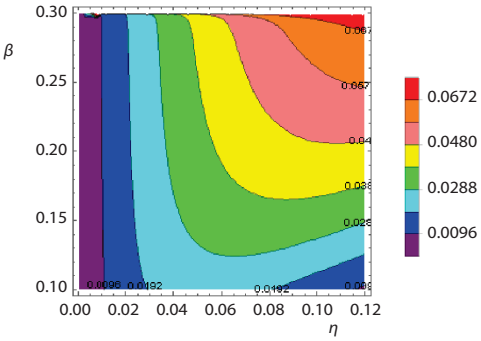

Figure 14. The β *vs.* x in SWCNT, when $n = 2$, Pr = 10.7, $S = 0.3$, $M = 0.3$, and $\phi = 0.01$

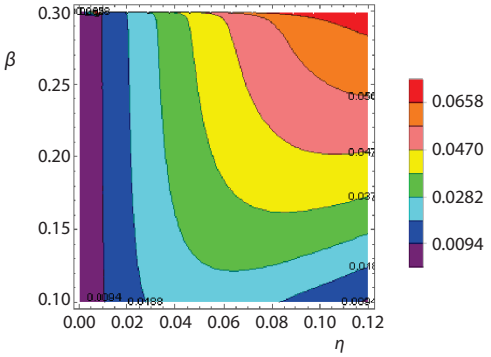

Figure 15. The β *vs.* x in MWCNT, when $n = 2$, Pr = 10.7, $S = 0.3$, $M = 0.3$, and $\phi = 0.01$

n, cause to decrease the flow motion as shown in fig. 4. In fact, the greater extent of *n* generating opposite force to drop the radial velocity, and this contrasting force is stronger in the MWCNT due to the closed compactness as compared to the SWCNT. The impact of the magnetic parameter, *M*, for both sorts of CNT (SWCNT/MWCNT) is presented in fig. 5. Keep in view greater values of the magnetic field, *M*, in engine oil based SWCNT and MWCNT reduce the radial velocity. The applied magnetic field B_0 creates induce current in the fluid to generate an opposing force (Lorentz force) which slow down the fluid velocity. The effect of β (thickness parameter) has been shown in fig. 6. The velocity field for both CNT falls using the larger values of β. In fact, the thin nanofluid layer enhances the velocity, pitch and a smaller amount of energy is needed for the motion of fluid-flow while the thick layer increases the resistance force to decline the radial velocity. Figure 7 exhibit the influence of nanoparticle, ϕ, on the streaming of CNT nanofluid. We found that by raising the value of nanoparticle, ϕ, results enhance the radial velocity, pitch for both MWCNT and SWCNT. Actually, the thin liquid film, the greater extent of ϕ upsurge the energy, transport and a special type of force that is present among the molecules called cohesive force which helps the velocity progress. This effect is more ridiculous in the SWCNT as compared to the MWCNT. The difference in the two types of the CNT is not clearly visible in the momentum boundary-layer. In fact, the finite domain of the liquid film, the high non-linearity of the problem and small volume fraction of the materials cause the difference between the two sorts of the CNT

The influence of ϕ *vs.* thermal boundary-layer has been exhibited in fig. 8. The thermal conductivity of the nanofluids depends on the particle volume fraction ϕ and the larger values of ϕ increases the temperature field. We noticed that decrease temperature profile and boost up the velocity, pitch for both MWCNT and SWCNT is gained in the range of $0 \leq \phi \leq 4\%$. The efficiency in the heat transfer enhancement of the SWCNT is more visible using the thermal boundary-layer as compared to the momentum boundary-layer. The unsteadiness parameter effect on the thermal boundary-layer has been depicted in fig. 9. The thickness of the boundary-layer enhances with higher extent of *S* consequence the cooling effect rises to decline the temperature field. The larger values of the non-linear stretching parameter, *n*, disturb the thin boundary-layer and produce a cooling effect to reduce the CNT nanofluid temperature as exhibited in fig. 10. Discussion of temperature distribution $\Theta(\eta)$ under the influence of Eckert number has been depicted in fig. 11. Eckert number consists of a dissipation term which creates viscous resistance result thermal conductivity enhance for its larger values and raise the temperature field. This effect is maximum in the SWCNT due to the rapid improvement in the thermal conductivity.

The influence of the physical parameters in the contour form according to the obtained results for the range of parameters have been shown in figs. 12-15 for the SWCNT and MWCNT, respectively.

The thermophysical properties of the SWCNT/MWCNT and engine oil nanofluids is presented in tab. 1. The thermal conductivity at different volume fraction for both types of CNT are displayed in tab. 2. The total residual error for the velocity and temperature fields using the

OHAM technique has been displayed in tab. 3. The obtained results are validated through numerical ND-solve method and the outputs are demonstrated in tab. 4. The influence of the physical constrants *vs.* $d^2f(0)/d\eta^2$ and $d\Theta(0)/d\eta$ have been shown in tabs. 5 and 6. The higher values of n, S, and β increasing $d^2f(0)/d\xi^2$. In fact, the larger amount of non-linearity, unsteadiness and thickness parameters, generate the opposing force which upsurges the skin friction. Increasing the thickness β and unsteadiness parameter S of the thin layer improving the opposite force to fluid-flow and producing cooling effects to improve the Nusselt number demonstrated in tab. 6. The greater values of Eckert number, generally increasing the thermal conductivity and as a result, decline the Nusselt number. Temperature profile enhances due to thermal diffusivity and thermal diffusivity increase by increasing Ecket number.

Table 1. The CNT and engine oil thermophysical properties

Physical properties	Engine oil	MWCNT	SWCNT
ρ [kgm^{-3}]	884	1600	2600
C_p [Jkg^{-1}K^{-1}]	1910	796	425
K [Wm^{-1}K^{-1}]	0.144	3000	6600

Table 2. Thermal conductivity of CNT *vs.* volume fraction ϕ

Volume fraction ϕ	0.0	0.01	0.02	0.03	0.04
k_{nf} for SWCNT	0.145	0.174	0.204	0.235	0.266
k_{nf} or MWCNT	0.145	0.172	0.2	0.228	0.257

Table 3. Individual averaged squared residual errors up to 20th order approximations, when $\beta = 1$, Pr = 6.7, $M = S$ = Re = Gr = 0.1, and $\phi = 0.01$

m	ε_m^f SWCNT	ε_m^f MWCNT	ε_m^Θ SWCNT	ε_m^Θ MWCNT
6	$5.0818 \cdot 10^{-4}$	$3.1464 \cdot 10^{-4}$	$2.0889 \cdot 10^{-5}$	$1.8315 \cdot 10^{-5}$
10	$1.5042 \cdot 10^{-6}$	$0.9451 \cdot 10^{-6}$	$3.2423 \cdot 10^{-7}$	$2.843 \cdot 10^{-7}$
14	$6.0317 \cdot 10^{-8}$	$5.1421 \cdot 10^{-8}$	$7.4416 \cdot 10^{-9}$	$6.8371 \cdot 10^{-9}$
20	$1.81121 \cdot 10^{-9}$	$0.9213 \cdot 10^{-9}$	$4.2869 \cdot 10^{-11}$	$3.5920 \cdot 10^{-11}$

Table 4. The OHAM and numerical (ND-solve) comparison for $f(\eta)$, when $\beta = 1$, Pr = 6.7, $M = S$ = Re = Gr = 0.1, and $\phi = 0.01$

η	OHAM	ND-solve
0.1	0.956789	1.000000
0.2	0.957369	0.992022
0.3	0.959098	0.985086
0.4	0.961942	0.979163
0.5	0.965847	0.974219
0.6	0.970737	0.970211

Table 5. Displays the effect of various parameters *vs.* drage force coefficient $-f''(0)$

n	S	β	$-f''(0)$ $\phi = 0.02$ SWCNT	$-f''(0)$ $\phi = 0.04$ SWCNT	$-f''(0)$ $\phi = 0.02$ MWCNT	$-f''(0)$ $\phi = 0.04$ MWCNT
2	0.1	0.3	0.03214	0.02921	0.02882	0.02601
3			0.04352	0.03911	0.03828	0.03722
4			0.05231	0.04371	0.04273	0.41673
	0.3		0.05529	0.04722	0.04629	0.04648
	0.5		0.05799	0.04968	0.04829	0.04722
		0.4	0.06429	0.05326	0.052428	0.05132
		0.5	0.07542	0.06420	0.06350	0.06219

Table 6. Displays the effect of various parameters *vs.* $-\Theta'(0)$

S	Ec	β	$-f'(0)$ $\phi = 0.01$ SWCNT	$-f'(0)$ $\phi = 0.02$ SWCNT	$-f'(0)$ $\phi = 0.01$ MWCNT	$-f'(0)$ $\phi = 0.02$ MWCNT
0.1	0.2	0.2	3.71635	6.13214	3.61754	4.72567
0.3			3.80213	6.16453	3.63243	4.81623
0.5			3.92217	6.20826	3.65346	4.95412
	0.3		3.60445	6.01308	3.1656	4.37524
	0.4		3.60255	6.0117	3.09636	4.1738
		0.3	4.42912	6.9238	4.01099	5.09259
		0.4	4.92398	7.21831	4.45952	6.18932

Conclusions

The flow of a liquid film comprising SWCNT/MWCNT engine oil based nanofluid over an unstable and flexible disc has been scrutinized in this article. The flexibility of the disc is considered non-linear. The positive values change from linear $n = 1$ to non-linear $n = 2, 3, 4,...$, which represent the non-linearity of the flexible disc. The thickness of the liquid film also differs from thinning $\beta = 0.01$ to thickening status $\beta = 0.2, 0.3, 0.4,..$, for the vigorous outcomes. The dissipation term and magnetic effects also implemented to the flow Pattern. The difference in the two types of the CNT is not clrealy visible in the momentum boundary-layer while this change is more evident in the thermal boundary-layer.

To accomplish the optimal values 20^{th} order of distortion for which the residual sum is minimized, we employed the provision of BVPh 2.0 package of OHAM technique. The summary of this article has been discussed in the following points.

- The appropriate range of the physical parameters has been observed using the BVPh 2.0 package.
- The thermal efficiency of the MWCNT is found less effective as compared to SWCNT.
- The extending of the disc in non-linear status decays the momentum and thermal boundary-layers for both sorts of CNT.
- The viscous dissipation enhancing the temperature distribution for its larger values and this consequence is more operative in the SWCNT.
- The larger values of the nanoparticle volume fraction decline the viscosity of the nanofluid and increases the fluid motion and temperature profile.

- The confrontation force increasing with the greater values of the magnetic parameter to decline the nanofluid motion.
- The increasing thickness of the liquid film produces the confrontation force to decline the velocity field and this consequence is very agree for the both sorts of CNT.

Numenclature

C_f – skin friction
k_f – thermal conductivity of base fluid
k_{nf} – thermal conductivity of the nanofluid
M – magnetic parameter
n – positive integer
Pr – Prandtl number
Re – Reynolds number
r – radial direction, [m]
S – unstiness parameter
T – temperature profile, [K]
T_{ref} – reference temperature, [K]
T_w – surface temperature, [K]
t – time
u – velocity in the r-direction, [ms^{-1}]
U_w – surface velocity, [ms^{-1}]
w – velocity in the z-direction, [ms^{-1}]
z – axis of the disk, [m]

Greek symbols

β – dimensionless thickness of the liquid film
η – similarity variable
μ – dynamic viscosity of the nanofluids
μ_f – dynamic viscosity of base fluid
ρ_f – density of the base fluid, [kgm^{-3}]
ρ_{nf} – density of the nanofluids
$(\rho C_p)_f$ – specific heat capacity of base fluid
$(\rho C_p)_{nf}$ – specific heat capacity of nanofluid
ϕ – solid particle volume fraction
φ – nanoparticle volume fraction

Competing interests

The authors state that they have no competing interests.

Acknowledgment

This project was funded by the Deanship of Scientific Research (DSR), King Abdulaziz University, Jeddah, SA under Grant No. KEP-18-130-19. The authors, therefore, acknowledge with thanks DSR technical and financial support.

References

[1] Oberlin, A., *et al*., Filamentous Growth of Carbon through Benzene Decomposition, *Journal Crystal Growth*, *32* (1976), 3, pp. 335-349
[2] Iijima, S., Helical Microtubules of Graphitic Carbon, *Nature*, *354* (199), 11, pp. 56-64
[3] Iijima, S., Ichihashi, T., Single-Shell Carbon Nanotubes of 1 nm Diameter, *Nature*, *363* (1993), 6, pp. 603-605
[4] Bethune, D. S., *et al*., Cobalt-Catalysed Growth of Carbon Nanotubes with Single-Atomic-Layer Walls, *Nature*, *363* (1993), 6, pp. 605-607
[5] To, C. W. S., Bending and Shear Moduli of Single-Walled Carbon Nanotubes, *Finite Elem Anal Des*, *42* (2006), 5, pp. 404-413
[6] Terrones, M., Science and Technology of the Twenty-First Century: Synthesis, Properties, and Applications of Carbon Nanotubes, *Annual Review Materials Research*, *33* (2003), 12, pp. 419-501
[7] De Volder, M. F. L., *et al*., Carbon Nanotubes: Present and Future Commercial Applications, *Science*, *339* (2013), 2, pp. 535-543
[8] Negin, C., *et al*., Application of Nanotechnology for Enhancing Oil Recovery, A Review, *Petroleum*, *2* (2016), 4, pp. 324-333
[9] Murshed, S. M. S., Nieto de Castro, C. A., Superior Thermal Features of Carbon Nanotubes-Based Nano-Fluids, A Review, *Renewable and Sustainable Energy Reviews*, *37* (2014), 9, pp. 155-167
[10] Zaidi, Z., *et al*., Convective Heat Transfer and MHD Analysis of Wall Jet Flow of Nanofluids Containing Carbon Nanotubes, *Eng. Comput.*, *34* (2017), 3, pp. 1-9
[11] Haq, R. U., *et al*., The MHD Pulsatile Flow of Engine Oil Based Carbon Nanotubes between Two Concentric Cylinders, *Results in Physics*, *7* (2017), Nov., pp. 57-68

[12] Xue, Q., Model for Thermal Conductivity of Carbon Nanotube-Based Composites, *Phys B Condens Matter*, 368 (2005), 11, pp. 302-307
[13] Garbadeen, I. D., *et al*., Experimental Study on Natural-Convection of MWCNT-Water Nanofluids in a Square Enclosure, *Int. Communications in Heat and Mass Transfer*, *88* (2017), 11, pp. 1-8
[14] Nasir, S., *et al*., Three-Dimensional Rotating Flow of MHD Single Wall Carbon Nanotubes over a Stretching Sheet in Presence of Thermal Radiation, *Applied Nanoscience*, *8* (2018), 6, pp. 1361-1378
[15] Rehman, A. U., *et al*., Effects of Single and Multi-Walled Carbon Nanotubes on Water and Engine Oil Based Rotating Fluids with Internal Heating, *Advanced Powder Technology*, *28* (2017), 9, pp. 1991-2002
[16] Ellahi, R., *et al*., Study of Natural-Convection MHD Nanofluid by Means of Single and Multiwalled Carbon Nanotubes Suspended in a Salt Water Solution, *IEEE Transactions on Nanotechnology*, *14* (2015), July, pp. 1-10
[17] Hayat, T., *et al*., Non-Darcy Flow of Water-Based Single (SWCNT) and Multiple (MWCNT) Walls Carbon Nanotubes with Multiple Slip Conditions due to Rotating Disk, *Results in Physics*, *9* (2018), June, pp. 390-399
[18] Farooq, S., *et al*., Mixed Convection Peristalsis of Corban Nanotubes with Thermal Radiation and Entropy Generation, *Journal of Molecular Liquids*, *250* (2018), Jan., pp. 451-467
[19] Aman, S., *et al*., Heat Transfer Enhancement in Free Convection fow of CNT Maxwell Nanofuids with Four Diferent Types of Molecular Liquids, *Scientific Reports*, *7* (2017), May, pp. 1-13
[20] Maxwell, J. C., *Electricity and Magnetism*, 3rd ed., Clarendon, Oxford, UK, 1904
[21] Jaffery, D. J., Conduction through a Random Suspension of Spheres, Proceedings of the Royal Society of London A, *Math. Phys. Sci*., *335* (1973), Nov., pp. 335-336
[22] Davis, R., The Effective Thermal Conductivity of a Composite Material with Spherical Inclusions, *Int. J. Thermophys*, *7* (1986), May, pp. 609-620
[23] Lu, S., Lin, H., Effective Conductivity of Composites Containing Aligned Spherical Inclusions of Finite conductivity, *Journal of Applied Physics*, *79* (1998), June, pp. 6761-6766
[24] Hamilton, R. I., Crosser, O. K., Thermal Conductivity of Heterogeneous Two-Component Systems, *Ind. Eng. Chem. Fundam*., *1* (1962), Aug., pp. 182-191
[25] Xue, Q., Model for Thermal Conductivity of Carbon Nanotube-Based Composites, *Phys B Condens Matter*, *368* (2005), Nov, pp. 302-307
[26] Shahzad, A., *et al.*, On the Exact Solution for Axisymmetric Flow and Heat Transfer over a Non-Linear Radially Stretching Sheet, *Chin. Phys. Letters*, *29* (2012), 8, 084705
[27] Hayat, T., *et al.*, Thermally Radiative Stagnation Point Flow of Maxwell Nanofluid Due to Unsteady Convectively Heated Stretched Surface, *Journal of Molecular Liquids*, *224* (2016), Dec., pp. 801-810
[28] Hayat, T., *et al*., The MHD Flow of Jeffrey Liquid Due to a Non-Linear Radially Stretched Sheet in Presence of Newtonian Heating, *Results in Physics*, *6* (2016), Oct., pp. 817-823
[29] Mustafa, M., *et al*., Analytical and Numerical Solutions for Axisymmetric Flow of Nanofluid Due to Non-Linearly Stretching Sheet, *Int. J. of Non-Linear Mechanics*, *71* (2015), May, pp. 22-29
[30] Wang, C. Y., Liquid Film on an Unsteady Stretching Surface, *Quart. Appl. Math*., *48* (1990), 4, pp. 601-610
[31] Gul, T., Scattering of a Thin Layer over a Non-Linear Radially Extending Surface with Magneto Hydro-Dynamic and Thermal Dissipation, *Surface Review and Letters*, *26* (2018), 1, pp. 1-7
[32] Ghani, F., *et al*., Unsteady Magnetohydrodynamics Thin Film Flow of a Third Grade Fluid over an Oscillating Inclined Belt Embedded in a Porous Medium, *Thermal Science*, *20* (2016), 5, pp. 875-887
[33] Gohar, T., *et al.*, The MWCNT/SWCNT Nanofluid Thin Film Flow over a Non-Linear Extending Disc: OHAM Solution, *Journal of Thermal Science*, *28* (2019),1, pp. 115-122
[34] Qasim, M., *et al*., Heat and Mass Transfer in Nanofluid over an Unsteady Stretching Sheet Using Buongiorno's Model, *Eur. Phys. J. Plus*, *131* (2016), Jan, pp. 1-16
[35] Wang, C. Y., Liquid Film Sprayed on a Stretching Cylinder, *Chem. Eng. Comm*., *193* (2006), 7, pp. 869-878
[36] Khan, N. S., *et al.*, Magneto Hydrodynamic Nanoliquid Thin Film Sprayed on a Stretching Cylinder with Heat Transfer, *Appl. Sci*., *7* (2017), Mar, pp. 271-296
[37] Alshomrani, A. S., Gul, T., A Convective Study of Al_2O3-H_2O and Cu-H_2O Nanoliquid Films Sprayed over a Stretching Cylinder with Viscous Dissipation, *Eur. Phys. J. Plus*, *132* (2017), Nov., pp. 495-512
[38] Liao, S. J.,The Proposed Homotopy Analysis Method for the Solution of Non-Linear Problems, Ph. D. Thesis, Shangai Jiao Tong University, Shanghai, China, 1992
[39] Liao, S. J., *Advances in the Homotopy Analysis Method*, Chapter 7, World Scientific Press, Singapore, 2013

[40] Zhao, Y., *et al.*, HAM-Based Mathematica Package BVPh 2.0 for Non-Linear Boundary Value Problems, in: *Advance in the Homotopy Analysis Method*, World Scientific Press, Singapore, 2014, Chapter 9, pp. 361-417
[41] Farooq, U., *et al*., Application of the HAM- Based Mathematica Package BVPh 2.0 on MHD Falkner-Skan Flow of Nanofluid, *Computers and Fluids*, *111* (16) (2015), Apr., pp. 69-75
[42] Ellahi, R., *et al*., Shape Effects of Spherical and Non-Spherical Nanoparticles in Mixed Convection Flow over a Vertical Stretching Permeable Sheet, *Mech. of Adv. Mater. and Structures*, *24* (2017), 15, pp. 1231-1238
[43] Ellahi, R., *et al*., Structural Impact of Kerosene-Al_2O_3 Nanoliquid on MHD Poiseuille Flow with Variable Thermal Conductivity: Application of Cooling Process, *Journal of Molec. Liquids*, *264* (2018), 15, pp. 607-615
[44] Gul, T., Ferdous, K., The Experimental Study to Examine the Stable Dispersion of the Graphene Nanoparticles and to Look at the GO-H_2O Nanofluid-flow between Two Rotating Disks, *Applied Nanoscience*, *8* (2018), 7, pp. 1711-1727
[45] Waqas, M., *et al*., A Theoretical Analysis of SWCNT-MWCNT and H_2O Nanoflids Considering Darcy-Forchheimer Relation, *Applied Nanoscience*, *9* (2019), July, pp. 1183-1191

Paper submitted: April 4, 2019
Paper revised: May 23, 2019
Paper accepted: May 31, 2019